

# **GCM Simulations of the Climate in the Central United States**

Kenneth E. Kunkel, Xin-Zhong Liang

Illinois State Water Survey

Champaign, Illinois

and participating CMIP2+ modeling groups<sup>1</sup>

---

<sup>1</sup> George Boer, Canadian Centre for Climate Modeling and Analysis, Victoria Canada

Byron Boville, National Center for Atmospheric Research, Boulder, CO USA

Curt Covey, Program for Climate Model Diagnosis and Intercomparison, Lawrence Livermore Laboratory, Livermore, CA USA

Hal Gordon, CSIRO Division of Atmospheric Research, Victoria, Australia

Jerry Meehl, National Center for Atmospheric Research, Boulder, CO USA

Josef Oberhuber, Max Planck Institute, Hamburg, Germany

Erich Roeckner, Max Planck Institute, Hamburg, Germany

Ron Stouffer, Geophysical Fluid Dynamics Laboratory, Princeton, MA USA

## Abstract

A diagnostic analysis of relationships between surface climate characteristics and various flow and scalar fields was used to evaluate 9 global coupled ocean-atmosphere general circulation models (CGCMs) participating in the Coupled-Model Intercomparison Project (CMIP). In order to facilitate identification of physical mechanisms causing biases, data from 21 models participating in the Atmospheric Model Intercomparison Project (AMIP) were also used for certain key analyses.

Most models reproduce basic features of the circulation, temperature, and precipitation patterns in the central US, including the pronounced seasonal cycles that are characteristic of this region and the general flow patterns, although no model exhibits small differences from observations for all characteristics in all seasons. Similar to the findings of other investigators performing global analyses, model ensemble means generally produce better agreement with observations than any single model. No single model is unambiguously superior to all other models.

A fall precipitation deficiency, found in all AMIP and CMIP models except HadCM3, appears to be related in part to slight biases in the flow on the western flank of the Atlantic subtropical ridge. In the model mean, the ridge at 850 hPa is displaced slightly to the north and to the west, resulting in weaker southerly flow into the central US.

The CMIP doubled-CO<sub>2</sub> transient runs show warming for all models and seasons, ranging from 2-7°C in summer to 6-9°C in winter with respect to their control simulations. These changes are larger than the natural variations that are observed in the 20<sup>th</sup> Century and the model variations in the control simulations. Precipitation changes with respect to the control simulations are mostly upward, but the magnitudes of changes are mostly less than the natural variations that are observed in the 20<sup>th</sup> Century and less than the model variations in the control simulations.

## **1. Introduction**

The coupled ocean-atmosphere general circulation models (CGCMs) that are the principal tools for assessment of potential anthropogenically-forced climate change exhibit a sizeable range of global sensitivities for temperature and precipitation. While global changes in key elements such as temperature and precipitation are important for some societal impacts (e.g. sea level rise), many of the potential impacts result from local and regional changes in climate. Such regional changes may differ substantially from zonally-averaged changes in the climate system. Furthermore, the uncertainties on a regional scale are greater than those on a global scale. Since most impacts are realized on the local and regional scale, these uncertainties are critical for assessing the impacts of future climate change and evaluating management strategies and policy options.

The Atmospheric Model Intercomparison Project (AMIP; Gates et al. 1998) and the Coupled Model Intercomparison Project (CMIP; Meehl et al. 2000), through their controlled experiments and worldwide participation of modeling groups, have proven to be very effective in improving understanding of uncertainties in model projections. Most assessments have taken a global perspective (e.g. Barnett et al. 2000; Lambert and Boer 2001; Covey et al. 2003). This needs to be the primary focus since global circulation systems must be simulated correctly to produce reasonable regional climates. However, regional analyses may also be valuable. Regional geographic/topographic features may have substantial influences on the regional climate but little influence globally. Also, such analyses can illuminate inconsistencies in large-scale circulation patterns that may be minor on a global scale, but important to some regions. Insights gained in this manner can be used to choose appropriate models for climate change assessments. For example, in a regional study of the Saharan desert Liu et al. (2002) analyzed 18 CMIP model simulations and identified 5 with accurate simulations of the present-day climatology. These 5 models were then used to assess the sensitivity of the Saharan climate to increasing global concentrations of greenhouse gases.

The principal objective of this study is to assess the ability of CGCMs to simulate the climate of the central United States, with the principal focus on precipitation. The region of study (delineated in Fig. 1) is one of the most productive agricultural regions in the world. It includes several major urban areas (including Chicago, the third largest in the US) and a portion of the drainage basin of the North American Great Lakes. Although precipitation is substantial (region-wide average annual precipitation is 980 mm), increasing population and economic growth may cause water shortages in the future. In the global depictions of CMIP results by Covey et al. (2003), this region is not highlighted as one where the simulated control climate exhibits large deviations from the observed climatology. The present analysis is more detailed, examining more fields and addressing the seasonal cycle.

For the central US, the most important source of water vapor is moisture transport from the Gulf of Mexico via southerly wind flow. Although water vapor can be transported by westerly winds from the Pacific Ocean into the central US, this contribution is minor because most of that water vapor is removed when the winds rise over the several mountain ranges to the west. Most precipitation is associated with the passage of extratropical cyclones (ECs). Thus, the location and the temporal variability of the mid-latitude upper-level jet stream are important climate features for this region. The Great Plains southerly low-level jet is another key feature, especially in summer. Our diagnoses focused on these dominant processes to assess and understand the performance of GCMs, including their climate biases as compared with observations and inter-model differences. The primary emphasis is on results from CMIP models since fully-coupled models are used to develop climate change projections. However, analysis of AMIP model data was also performed and selected AMIP results are included to help better understand the physical mechanisms for model biases.

## 2. Data

The Atmospheric Model Intercomparison Project (AMIP, Gates et al. 1998) was undertaken to provide a framework for comparisons of atmospheric GCMs (AGCMs). This study analyzed an historical simulation of the period 1979-1995 for the AMIP II experiment. The sea surface temperatures (SSTs) were specified as monthly mean variations based on actual observations. In this experiment, all AGCMs use the same “perfect” ocean surface conditions to determine the fluxes of heat, moisture, and momentum needed to drive the atmosphere. (“Perfect” here refers to the use of actual data, as compared to the use of ocean model output which usually contain some biases.) Each model also used the same values of atmospheric CO<sub>2</sub> concentration (345 parts per million) and solar constant (1365 W m<sup>-2</sup>). Specification of the land surface and inclusion of the radiative effects of other greenhouse gases and aerosols was left up to each modeling group and thus varied among models. Data from this experiment include 21 AGCMs, all of which were used for this diagnostic analysis.

The Coupled Model Intercomparison Project (CMIP, Meehl et al. 2000) is similar to AMIP except that the models are fully coupled GCMs. The experiment analyzed in this study is denoted as CMIP2. This consisted of a control run of at least 80 years duration in which greenhouse gas concentrations were fixed followed by a transient run of at least 80 years duration in which CO<sub>2</sub>-equivalent concentration increases at the rate of 1%/year. A variety of methods are used to determine the initial state of the atmosphere and ocean at the beginning of the control run; these are briefly described at

<http://www-pcmdi.llnl.gov/modeldoc/cmip/table2.html>. In both runs, the solar constant and land use did not change and the inclusion of aerosol effects and other greenhouse gases varied among models. In the transient run, CO<sub>2</sub>-equivalent concentrations reach a doubling compared to initial concentrations around year 70. Data from this experiment include 9 CGCMs. Several of the models participating in both AMIP and CMIP use the same or a very similar atmospheric component. The particular dataset used here is referred to as “CMIP2+” which is an extension of CMIP2 with an expanded set of fields at monthly or shorter time resolution.

Table 1 lists the CMIP CGCMs used in this study along with certain model characteristics and key references. Since these models contain an interactive ocean component and ocean surface conditions are computed by the model rather than specified, the SSTs can differ among models and from observations. Six models use flux adjustment to minimize climate drift while the other three do not.

There are some differences between the CMIP and AMIP experiments. In the AMIP experiment, the CO<sub>2</sub>-equivalent concentration was fixed at 345 ppm while in the CMIP control simulation it varies among the models from 290 to 355 ppm. Likewise, the solar constant was fixed in AMIP at 1365 W m<sup>-2</sup> while in CMIP it varies from 1365 to 1370 W m<sup>-2</sup>.

All model data were obtained through the web-based infrastructure of the Program for Climate Model Diagnosis and Intercomparison. Two major sources of observational data were used. For comparison of wind, humidity and pressure patterns, the NCEP-DOE AMIP II reanalysis (R-2; Kanamitsu et al. 2002) was used. For comparison of surface air temperature and precipitation, data from the National Weather Service's cooperative observer network, as archived in the TD-3200 data set of the National Climatic Data Center, was used.

### **3. Results**

For both AMIP and CMIP, various climate elements were available as monthly means at each grid point with varying grid spacings (see Tables 1 and 2). The following climate elements were chosen for diagnostic analysis: precipitation, surface air temperature, wind and pressure level height at 850 and 200 hPa. The analysis at 850 hPa was chosen because much of the moisture transport into the central US from the Gulf of Mexico occurs at and below this level. The analysis at 200 hPa was chosen because this level is near the core of the upper level jet stream which is an essential feature associated with extratropical cyclone activity.

In the following discussion, the observed fields are first presented; these provide the basis for the diagnostics presented in some of the graphs. This is followed by an analysis of precipitation and

temperature in the control simulations. Finally, a brief analysis of temperature and precipitation changes in the transient simulations is presented.

#### *a. Observed fields*

Figure 2 shows observed average flow patterns at 850 hPa. In winter, the average flow in the central US is from the west and northwest. Because flow from the Gulf of Mexico does not usually penetrate into the central US, the winter season is relatively dry. During the spring, summer, and fall, the mean flow is still from the west, but it is part of a curved pattern that originates in the Gulf of Mexico, moves across Texas, and curves northeastward into the central US. Thus, moisture is more abundant in these three seasons. This pattern is most pronounced in the summer, the wettest season.

At 200 hPa, the average flow is westerly over the central U.S in all seasons (Fig. 3). The average position of the jet stream is to the south of the central US in winter and spring, over the region in fall, and to the north in summer. Highest wind speeds occur in the winter when the north-to-south temperature gradient is largest.

An analysis was undertaken in which a time series of monthly precipitation anomalies averaged for the central US region was correlated with time series of the meridional wind component at 850 hPa for each grid point. Maps of the spatial pattern of correlations (Fig. 4) show that precipitation anomalies are highly correlated with southerly flow over the Mississippi River basin at 850 hPa. Correlations of greater than 75% are seen for distinct broad areas. There are slight variations by season with a westward shift in the pattern in the summer. However, high correlations are seen in all seasons from central Texas to Louisiana.

A similar analysis was performed for the zonal wind component at 200 hPa. High correlations are found generally in a belt from California to the Great Lakes (Fig. 5). This reflects the average location of the jet stream during periods when extratropical cyclones are causing precipitation over the central U.S. There are some seasonal variations in the strength of the correlations, but the location of the high correlations is about the same in all seasons, although correlations in the central US are quite low in the fall.

The results shown in Figs. 4 and 5 were used to identify 3 regions for analysis of the model data (Fig. 1). Although all seasons were considered, the summer season was given the highest weight because of its importance to the widespread non-irrigated agriculture of the region. The box covering eastern Texas and Oklahoma corresponds to an area of high correlations at 850 hPa (Fig. 4) and reflects the importance of low level moisture transport from the Gulf of Mexico; this area will be referred to as the “LLJ” (low level jet) region. The box covering Iowa and portions of adjacent states corresponds to an area of high correlations at 200 hPa (Fig. 5) in winter, spring, and summer; this will be referred to as the “IA” (Iowa) region. The box covering California and Nevada corresponds to a second area of high correlations at 200 hPa (Fig. 5); this area will be referred to as the “CA” (California) region.

#### *b. Precipitation*

Annual precipitation for the control runs of CMIP models and for observations is shown in Fig. 6. In the CMIP control runs, the SSTs are calculated by the model and the CO<sub>2</sub> concentration is fixed. Thus, it is not obvious what historical observational period should be chosen to compare with the model simulations. In the case of the AMIP simulations, the SSTs are specified from the period 1979-1995 and thus a direct comparison with observations for that same period is appropriate. For convenience, we have chosen the same 1979-1995 period for comparison with CMIP results, but it should be recognized that small differences between a CMIP model and observations may not be physically significant. Model values of annual mean precipitation range from 2.0 to 3.2 mm/day, compared to an observed value of 2.7 mm/day. The model mean value is 2.6 mm/day. Seven of the 9 models are within 10% of observations. The CSIRO is about 25% drier than observed and the HadCM3 is about 20% too wet. The comparison of seasonal precipitation (Fig. 7) indicates some inconsistencies across seasons. In winter, all models are within 25% of observed except for HadCM3 which is about 50% wetter than observed. In spring, all models are close to, or wetter than, observed. The GFDL and HadCM3 are more than 20% wetter than observed. In summer, 5 of the 9 models were within 10% of observed. The CSIRO and GFDL are 20% or more drier than observed,

while the PCM and CSM are about 15% wetter than observed. All models but one are substantially drier than observed in fall, the only exception being the HadCM3. The CMIP model mean values are very near the observed values, except for fall (model mean of 2.0 mm/day compared to an observed value of 2.8 mm/day).

The negative bias in fall precipitation exhibited by 8 of the 9 CMIP models is also found in the AMIP simulation (Fig. 7). In this case, all 21 AMIP models exhibit a negative bias and the AMIP model mean is 1.8 mm/day. Thus, this model bias presumably originates in the atmospheric component.

The mean values for the southerly component of the 850 hPa wind speed in the LLJ region are shown in Fig. 8 for CMIP models and observations. All models produce the correct seasonal cycle with a maximum in the summer and a minimum in the winter. The amplitudes of the seasonal cycle are similar to observations for many models. One notable exception is ECHO whose seasonal amplitude of  $1.6 \text{ m s}^{-1}$  is much less than the observed value of  $4.8 \text{ m s}^{-1}$ . Both CCCMA and HadCM2 have somewhat larger amplitudes than observed. The model mean values are very close to observed in spring and summer, slightly more negative in winter, and smaller in fall. The weaker southerly flow in fall may be related to the negative precipitation biases.

For specific humidity at 850 hPa in the LLJ region (Fig. 9), the CMIP models generally simulate the seasonal cycle with a minimum in winter and a maximum in summer. Although magnitudes are generally within 15% of observations, the CCCMA and HadCM3 are more than 15% moister in spring, summer and fall. The model mean values are very close to observed in all seasons.

Interannual correlations between central US precipitation and the southerly wind component at 850 hPa in the LLJ region were calculated for CMIP models by season (Fig. 10). The values for the models are within 20% (this is the absolute, not relative, difference, the convention used here for all correlation graphs) of observed in the winter except for HadCM2. In the spring, three models (ECHO, PCM, and HadCM2) differ from observations by more than 30%. In summer, CCCMA, HadCM2, and HadCM3 differ from

observations by more than 40%. In fall, the ECHAM4 differs by about 40% and HadCM2 by about 55%. The model mean values are lower than observed in all seasons, most notably in summer and fall.

Interannual correlations for the IA region between Central US precipitation and the westerly wind component at 200 hPa are shown in Fig. 11 for CMIP models. In winter, CSM and HadCM2 differ from the observed correlation by more than 20%. In spring, ECHO is about 40% lower than observed. In summer, all models have somewhat lower correlations than observed. In fall, all correlations are within 20% of observed. The model mean values are relatively close to observed except for summer where the model mean value of 36% is considerably smaller than the observed value of 68%.

Interannual correlations for the CA region between central US precipitation and the westerly wind component at 200 hPa are shown in Fig. 12 for CMIP models. There is more variability in the model results than was found for the LLJ and IA regions, perhaps reflecting the greater distance from the region of interest. In winter, four models (ECHO, ECHAM4, HadCM2, and HadCM3) have correlations at least 20% more than observed. In spring, the correlations for ECHO and PCM are at least 20% less than observed. The CSM and CCCMA have correlations at least 30% less than observed in summer. In fall, the ECHAM4 and PCM correlations are at least 20% less than observed. The model mean values differ from observed from observed values by about 20% except in fall where the difference is only 3%.

### *c. Temperature*

The comparison of mean annual temperature in CMIP models, shown in Fig. 13, indicates that all models are within 1.5°C of the 1979-1995 observed mean. Model values range from 9.1 to 12.3°C. The model mean value of 10.4°C compares favorably with the observed value of 10.7°C. Somewhat larger differences are observed for the seasonal values (Fig. 14), although the amplitude of the seasonal cycle is similar to observed for most models. The HadCM3 and CSIRO models exhibit a somewhat larger amplitude in the seasonal cycle with colder temperatures in the winter and warmer temperatures in the

summer compared to observations. The CCCMA model exhibits very cold temperatures (about 5°C less than observed) in the spring, but is within 2°C of observations in the other 3 seasons. The model mean shows a seasonal cycle whose amplitude is slightly larger (by 1.3°C) than observed, a result consistent with Covey et al. (2000).

#### *d. Model Sensitivity to Enhanced Greenhouse Gas Forcing*

The sensitivity of CMIP models to certain changes in forcing was analyzed by examining years 65-75 in the transient simulation and comparing precipitation rates and temperatures for this period with the last 30 years of the control simulation. Seasonal results are presented in terms of differences between the two periods (Fig. 15 and 17).

For precipitation (Fig. 15), in winter 5 of the 9 models show little change while the other 4 exhibit increases of 0.2-0.4 mm/day. In spring, 4 of the 9 models show changes of less than 0.2 mm/day while the other 5 exhibit increases of 0.2-0.5 mm/day. There is more variability in summer. The ECHO, HadCM3 and ECHAM4 show increases of more than 0.2 mm/day. By contrast, the CCCMA and HadCM2 show sizeable decreases of 0.6 mm/day. In fall, 5 of the 9 models show changes of less than 0.2 mm/day; 3 show decreases of more than 0.2 mm/day while HadCM3 exhibits an increase of about 0.3 mm/day. How do these changes compare to precipitation variations that would occur naturally, that is, without enhanced greenhouse warming? This question was investigated by performing a more detailed analysis of the control simulations of the CMIP models. The length of the control simulation varied among models, but was at least 79 years in length. Time series of seasonal precipitation were smoothed with a 11-year running average filter. The maximum, minimum, and mean values among these running windows were identified and plotted (Fig. 16). The smoothing window of 11 years was chosen to match the length of the analyzed portion of the transient simulation plotted in Fig. 15. A similar analysis was performed on observed data for the period 1900-1999. The maximum and minimum values are in the range of 0.2-0.6 mm/day above and

below the mean for both models and observations except for HadCM2 in the summer with values of 0.8 mm/day. When comparing these variations to the transient changes shown in Fig. 15, in most cases the transient changes are within the envelope of the natural variations summarized in Fig. 16. These results suggest that the transient simulations' changes due to the specified anthropogenic forcing are in most cases not unambiguously different than natural variations observed in the 20<sup>th</sup> Century or simulated in the control runs.

For temperature (Fig. 17), all models show warming in all seasons. The results are rather consistent for winter, the models being in the range of about 6-9°C warming. In spring, there is more variation, the models ranging from 3 to 9°C warming. In summer, warming is in the range of 2-7°C. In fall, warming ranges from about 4°C to slightly more than 7°C. As was done for precipitation, an 11-yr running average filter was applied to the temperature time series of the control simulations to examine the internal variations of the models and to observed temperatures for 1900-1999. The maximum and minimum values of the 11-yr running average time series (Fig. 18) indicate variations about the average of 0.4-1.4°C for both models and observations. All of the temperature increases found in the transient simulations exceed the range of internal model variations found in the control simulations and observed variations, suggesting that warming in the models is unambiguously due to the models' anthropogenic forcing.

## 5. Summary and Explanation for Model Biases

The major characteristics of the model simulations are:

- (1) Annual precipitation in CMIP models is within 10% of observed in 7 of the 9 available models. The CSIRO and HadCM3 models are 25% drier and 20% wetter than observed, respectively. The seasonal precipitation cycle in CMIP models ranges from 1.4 to 2.4 mm/day, compared to an observed value of 1.8 mm/day. Except for the fall season, the magnitudes of seasonal precipitation are within 0.5 mm/day of

observed in most cases. However, each model exhibits a difference of greater than 20% in at least one season. All CMIP models but one (HadCM3) and all AMIP models are drier than observed in the fall.

(2) Mean annual temperature in the CMIP models is within 1.5°C of observed for all models. The amplitude of the seasonal cycle varies from 23.1 to 30.5°C, compared to an observed value of 25.1°C.

(3) In the transient simulations, there is a mix of conditions at the time of CO<sub>2</sub> doubling, with some models simulating higher precipitation and others simulating decreased precipitation compared to the control simulation. However, in almost all cases the changes are smaller than the natural variations observed in the control simulations. In the transient simulations, all models show substantial warming, compared with the control simulation, in all seasons with the typical pattern of maximum warming in the winter and minimum warming in the summer. Overall, HadCM3 is the warmest model while CSM and PCM are the coolest. In almost all cases, at the time of CO<sub>2</sub>-doubling the temperature changes (2-9°C) are larger than the variations in the control simulations and in the observations (0.4-1.4°C).

(4) The seasonal cycle of southerly wind flow at 850 hPa in the LLJ region exhibits a cold season minimum and warm season maximum in all CMIP models. The amplitude of the seasonal cycle varies from 1.7 to 8.8 m s<sup>-1</sup>, compared to the observed value of about 4.9 m s<sup>-1</sup>. The seasonal cycle of specific humidity at 850 hPa in the LLJ region exhibits a cold season minimum and warm season maximum in all CMIP models. The amplitude of the seasonal cycle varies from 0.005 to 0.011 kg H<sub>2</sub>O/kg air, compared to an observed value of 0.007 kg H<sub>2</sub>O/kg air.

(5) The correlations between precipitation and southerly flow at 850 hPa in the LLJ region are within 25% of observed in the winter for all CMIP models except HadCM2. In the other 3 seasons, differences of greater than 25% are found for several models. The CSM is the only model within 25% of observations in all four seasons. For westerly flow at 200 hPa in the IA region, the correlations are within 25% of values for several models. However, correlations are lower than observed in the summer for all models. The

HadCM2 has correlations within 25% of observed in all four seasons. For westerly flow at 200 hPa in the CA region, no model is within 25% of observed values in all four seasons.

These findings show that the ability of GCMs to simulate the regional climate of the central US exhibits considerable model-to-model variability. For precipitation-related variables, most models reproduce certain basic features of the regional climate. The general shape of the seasonal cycle is simulated. Most models are able to simulate the seasonal changes in southerly flow from the Gulf of Mexico and the atmospheric water vapor content there and in the central US. These results reflect the models' ability to reproduce the large-scale circulation patterns and basic processes of the hydrologic cycle. There is more variation among the models in reproducing the connections between specific circulation patterns and precipitation episodes in the central US.

Model mean (averages of all models; MM) maps were produced to provide additional insights. Both Lambert and Boer (2001) and Covey et al. (2003) presented global MM maps of selected fields for CMIP simulations. The MM maps for 850 hPa and 200 hPa flow for the 30-year control CMIP period (Figs. 19 and 20) are in impressively close correspondence with the observed patterns (Figs. 3 and 4). This is similar to the global scale results of Lambert and Boer (2001) who found that the model mean provided an overall best comparison with climatology. However, there are subtle differences that may be important for precipitation processes in the central US. In the winter, the minimum 850 hPa wind speed in the Gulf of Mexico extends further to the west to the Texas coast. In the spring, the 850 hPa comparison is quite close. In the summer, the 850 hPa minimum is shifted to the east and the high wind speed core over Texas is weaker and broader compared to the observed. This may explain in part the more variable correlation patterns in the models (Fig. 10). In the fall, the 850 hPa minimum is shifted to the north and extended to the west. This shift in the fall may explain the low precipitation because the MM pattern would lead to an overall weaker advection of moisture from the Gulf of Mexico. At 200 hPa, the location of the spring

maximum wind speed is slightly to the north of observed. In summer, the 200 hPa maximum is somewhat higher than observed. The 200 hPa comparison for fall and winter is quite close.

The similarity of AMIP and CMIP results suggests that precipitation biases are principally a consequence of atmospheric processes. In the following analysis, AMIP model results are presented because the larger number of models provides a more robust statistical description. MM maps were prepared for the correlation between precipitation biases and wind flow biases (model minus observed monthly means averaged over all years) for AMIP models to help identify mechanisms causing the precipitation biases. In the following discussion they are compared with the correlations maps between observed precipitation and observed wind shown in Figs. 4 and 5, even though the MM maps show correlations among models for climatological mean biases while Fig. 4 and 5 show interannual correlations in the observed data. If the physical representation of precipitation processes is basically correct, then we might expect that model-to-model differences may be similar to the temporal variations occurring in the observed pattern. This approach has been successfully used by Liang et al. (2001a) to identify physical mechanisms for GCM biases in simulating the China monsoon system. For southerly flow at 850 hPa (Fig. 21), the models on average have positive correlations in the same general regions as are found in the observed correlation maps (Fig. 4) during winter, spring, and fall. This suggests that model precipitation biases are related to biases in the 850 hPa southerly flow in these seasons. In summer, the composite high correlations in the eastern portion of the central US are located in the same area as observed high correlations (Fig. 4), but the composite correlations are near zero over Texas, an area of high correlations in the observed map (Fig. 4). This may indicate unrealistic or inconsistent representation of the LLJ-central US precipitation relationship among GCMs. MM maps for the correlation between precipitation and westerly flow at 200 hPa (Fig. 22) show a mixed picture. In the winter, the composite bias correlations are high over the eastern subtropical Pacific and low over the northwest US, in different positions than the observed maximum over the Great Lakes and minimum over the Gulf of Mexico. In the spring, the minimum over

the northwest and maximum over the southwest are in similar positions to observed correlations, but the observed maximum extends into the Great Lakes region, a feature not seen in the bias correlations. In the summer, the maximum over the central U.S. and the minimum over the subtropics are in similar positions to the observed correlation pattern. In the fall, the minima over the northwest and the southeast are in similar positions to observed correlation minima, but the observed weak maximum over the central U.S. is not seen in the bias correlation map. MM maps of correlations were not produced for CMIP because of the small number of models available resulting in low statistical reliability.

The number of basic similarities between Figs. 4 and 5 and 21 and 22 suggest that fundamental physical processes are being simulated correctly in a general sense. The differences between Figs. 4 and 5 and 21 and 22 may arise from several sources, in particular the representation of topography and convection (e.g., Liang et al. 2003). The mountain chains in the western US play an important role in key features such as the LLJ and the development and path of ECs, especially in summer. The topographic variations in GCMs are a rather crude approximation of reality because of their coarse spatial resolution. The parameterization of the precipitation processes occurring within a grid box is known to be one of the most challenging aspects of climate system modeling because many processes, such as individual thunderstorm cells, are of a much smaller scale than the size of a grid, yet are extremely important to the magnitude of precipitation.

## 6. Conclusions

This analysis, primarily focused on precipitation, used diagnostic relationships between surface climate characteristics and various flow and scalar fields as the basis for model evaluation. This evaluation included qualitative descriptions of the comparison between models and observations for geographical distributions of various key variables. In addition, indices of flow and water vapor content were calculated

for several key regions and correlated with precipitation anomalies in the central US to provide a concise quantitative measure of model performance and better understanding of model biases.

Most models (both CMIP and AMIP) reproduce basic features of the circulation, temperature, and precipitation patterns in the central US, including the pronounced seasonal cycles that are characteristic of this region and the general flow patterns, although no model exhibits small differences from observations for all characteristics in all seasons. Similar to the findings of other investigators performing global analyses, model ensemble means generally produce better agreement with observations than any single model. No single model is unambiguously superior to all other models. Among CMIP models, the CSIRO and HadCM3 models exhibit the largest precipitation biases. The HadCM3 is also the coolest CMIP model.

The fall precipitation deficiency, common to all AMIP and CMIP models except HadCM3, appears to be related in part to slight biases in the flow on the western flank of the Atlantic subtropical ridge. In the model mean, the ridge at 850 hPa is displaced slightly to the north and to the west, resulting in weaker southerly flow into the central US. We hope that identification of this bias will motivate investigations of its causes and improvements in model simulations of this important feature.

One particular area of application of these results relates to the use of global models to drive regional climate models (RCMs). Regional climate change assessments often utilize dynamic downscaling with RCMs to produce the spatial detail needed for impacts models, an approach used by two of the authors (Liang et al. 2001b; Liang et al. 2003) and others. The substantial computer resources required for RCM simulations usually limit the number of global models can be used to provide boundary conditions for RCM simulations. The findings of this study can provide a foundation for the choice of global models. A strategy worthy of consideration is to choose models whose performances are complementary and who as a set include at least one model providing a good simulation of the current climate in all 4 seasons. In the case where computer resources limit studies to the use of 2 global models, an examination of Figs. 6 and 7 suggest a pairing of HadCM3 with any of the other models except CSIRO. The HadCM3 and CSIRO stand

out for rather large biases in precipitation. However, the HadCM3 is the only model to produce enough precipitation in the fall. On this basis alone, the model warrants consideration for use in regional studies of the central US. These conclusions for choice of driving CGCMs apply only to the central U.S. Studies of other regions may find that other choices are more appropriate.

## 8. Acknowledgements

This work was partially supported by the Illinois Board of Higher Education (IBHE) and the United States Environmental Protection Agency (USEPA) under award number EPA RD-83096301-0. Data analysis and graphic preparation were performed by Li Li and Heng Liu. The authors thank G. Meehl and C. Covey for their assistance in model data access. We acknowledge LLNL/PCMDI for making the AMIP and CMIP results available. The views expressed herein are those of the authors and do not necessarily represent those of the IBHE, USEPA, or the Illinois State Water Survey.

## 9. References

- Barnett, T. P., 1999: Comparison of near-surface air temperature variability in 11 coupled global climate models. *J. Climate*, **12**, 511-518.
- Boer, G.J., G. Flato, and D. Ramsden, 2000: A transient climate change simulation with greenhouse gas and aerosol forcing: projected climate to the twenty-first century. *Climate Dyn.*, **16**, 427-450.
- Boville, B.A., and P.R. Gent, 1998: The NCAR Climate System Model, Version One. *J.Climate*, **11**, 1115-1130.
- Covey, C., A. Abe-Ouchi, G.J. Boer, B.A. Boville, U. Cubasch, L. Fairhead, G.M. Flato, H. Gordon, E. Guilyardi, X. Jiang, T.C. Johns, H. Le Treut, G. Madec, G.A. Meehl, R. Miller, A. Noda, S.B. Power, E. Roeckner, G. Russell, E. K. Schneider, R.J. Stouffer, L. Terray, and J.-S. von Storch,

- 2000: The seasonal cycle in coupled ocean-atmosphere general circulation models. *Clim. Dyn.*, **17**, 775-787.
- Covey, C., K.M. AchutaRao, U. Cubasch, P. Jones, S.J. Lambert, M.E. Mann, T.J. Phillips, K.E. Taylor, 2003: An overview of results from the Coupled Model Intercomparison Project. *Global and Planetary Change*, **37**, 103-133.
- Delworth, T.L., and T.R. Knutson, 2000: Simulation of early 20th century global warming. *Science*, **287** (5461), 2246-2250.
- Flato, G.M., G.J. Boer, W.G. Lee, N.A. McFarlane, D. Ramsden, M.C. Reader, and A.J. Weaver, 2000: The Canadian Centre for Climate Modelling and Analysis global coupled model and its climate. *Climate Dyn.*, **16**, 451-467.
- Flato, G.M., and G.J. Boer, 2001: Warming asymmetry in climate change simulations. *Geophys. Res. Lett.*, **28**, 195-198, 10.1029/2000GL012121.
- Gates, W. L., J. Boyle, C. Covey, C. Dease, C. Doutriaux, R. Drach, M. Fiorino, P. Gleckler, J. Hnilo, S. Marlais, T. Phillips, G. Potter, B. Santer, K. Sperber, K. Taylor and D. Williams, 1998: An overview of the results of the Atmospheric Model Intercomparison Project (AMIP I). *Bull. Amer. Meteor. Soc.*, **73**, 1962-1970.
- Gordon, C., C. Cooper, C.A. Senior, H.T. Banks, J.M. Gregory, T.C. Johns, J.F.B. Mitchell, and R.A. Wood, 2000: The simulation of SST, sea ice extents and ocean heat transports in a version of the Hadley Centre coupled model without flux adjustments. *Climate Dyn.*, **16**, 147-168.
- Gordon, H.B., and S.P. O'Farrell, 1997: Transient climate change in the CSIRO coupled model with dynamic sea ice. *Mon. Wea. Rev.*, **125**, 875-907.

Hirst, A.C., S.P. O'Farrell, And H.B. Gordon, 2000: Comparison of a coupled ocean-atmosphere model with

and without oceanic eddy-induced advection. 1. Ocean spin-up and control integrations. *J. Climate*, **13**, 139-163.

Johns, T.C., R.E. Carnell, J.F. Crossley, J.M. Gregory, J.F.B. Mitchell, C.A. Senior, S.F.B. Tett, and R.A. Wood, 1997: The second Hadley Centre coupled ocean-atmosphere GCM: Model description, spinup and validation. *Climate Dyn.*, **13**, 103-134.

Kanamitsu, M., W. Ebisuzaki, J. Woollen, S.-K. Yang, J.J. Hnilo, M. Fiorino, and G.L. Potter, 2002: The NCEP-DOE AMIP-II reanalysis (R-2). *Bull. Amer. Meteor. Soc.*, **83**, 1631-1643.

Lambert, S.J. and G.J. Boer, 2001: CMIP1 evaluation and intercomparison of coupled climate models. *Clim. Dyn.*, **17**, 83-106.

Liang, X.-Z., K.E. Kunkel, and A.N. Samel, 2001a: Development of a regional climate model for U.S. Midwest applications. Part 1: Sensitivity to buffer zone treatment. *J. Climate*, **14**, 4363-4378.

Liang, X.-Z., L. Li, K.E. Kunkel, M. Ting, and J. X. L. Wang, 2003: Regional climate model simulation of U.S. precipitation during 1982-2002 Part I: Annual cycle. *J. Climate*, submitted.

Liang, X.-Z., W.-C. Wang, and A.N. Samel, 2001b: Biases in AMIP model simulations of the east China monsoon system. *Climate Dynamics*, **17**, 291-304.

Liu, P., G.A. Meehl, and G. Wu, 2002: Multi-model trends in the Sahara induced by increasing CO<sub>2</sub>. *Geophys. Res. Lett.*, **29**, 1881, doi: 10.1029/2002GL015923.

Meehl, G.A., G.J. Boer, C. Covey, M. Latif, and R.J. Stouffer, 2000: The Coupled Model Intercomparison Project (CMIP). *Bull. Amer. Meteor. Soc.*, **81**, 313--318.

Roeckner, E., J.M. Oberhuber, A Bacher, M. Christoph, and I. Kirchner, 1996: ENSO variability and atmospheric response in a global coupled atmosphere-ocean GCM. *Climate Dyn.*, **12**, 737-754.

Washington, W.M., J.M. Weatherly, G.A. Meehl, A.J. Semtner, Jr., T.W. Bettge, A.P. Craig, W.G. Strand, J. Arblaster, V.B. Wayland, R. James, and Y. Zhang, 2000: Parallel Climate Model (PCM) control and transient simulations. *Climate Dyn.*, **16**, 755-774.

Table 1. Characteristics of CMIP Models

	Flux Adjustment	Control Run CO <sub>2</sub> (ppm)	Solar Constant (Wm <sup>-2</sup> )	No. Vertical Levels	Bottom, Top (hPa)	Key References
CCCMA	Yes, heat, water	330	1370	10	980, 5	Flato et al. 2000 Flato and Boer, 2001 Boer et al. 2000
NCAR CSM	No	355	1367	18	992, 3	Boville and Gent 1998
CSIRO	Yes, heat, water, momentum	330	1367	9	979, 21	Gordon and O'Farrell, 1997; Hirst et al., 2000
ECHAM-OPYC	Yes, heat, water	353	1365	19	996, 10	Roeckner et al., 1996
ECHO	Yes, heat, water			19	996, 10	
GFDL	Yes, heat, water	360	1365	14	997, 15	Delworth and Knutson, 2000
HADCM2	Yes, heat, water	322.6	1365	19	997, 5	Johns et al., 1997
HADCM3	No	289.6	1365	19	997, 5	Gordon et al., 2000
DOE PCM	No	355	1367	18	992, 3	Washington et al ., 2000

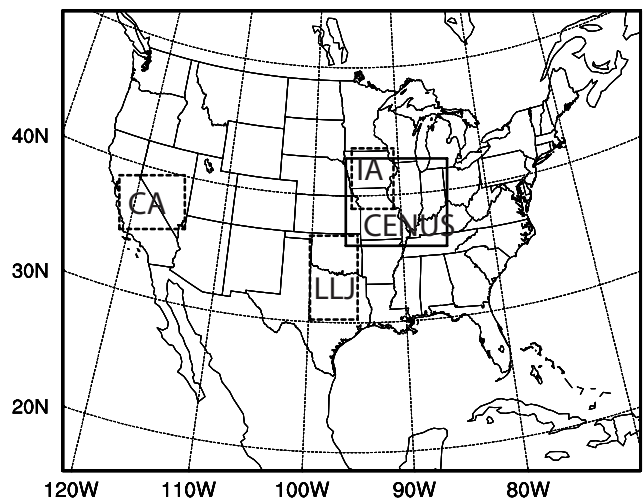


Figure 1. Solid box outlines the central U.S. (CENUS) area of study. Dashed boxes outline three areas for which indexes were calculated: a low-level jet area (LLJ), an Iowa area (IA), and a California area (CA).

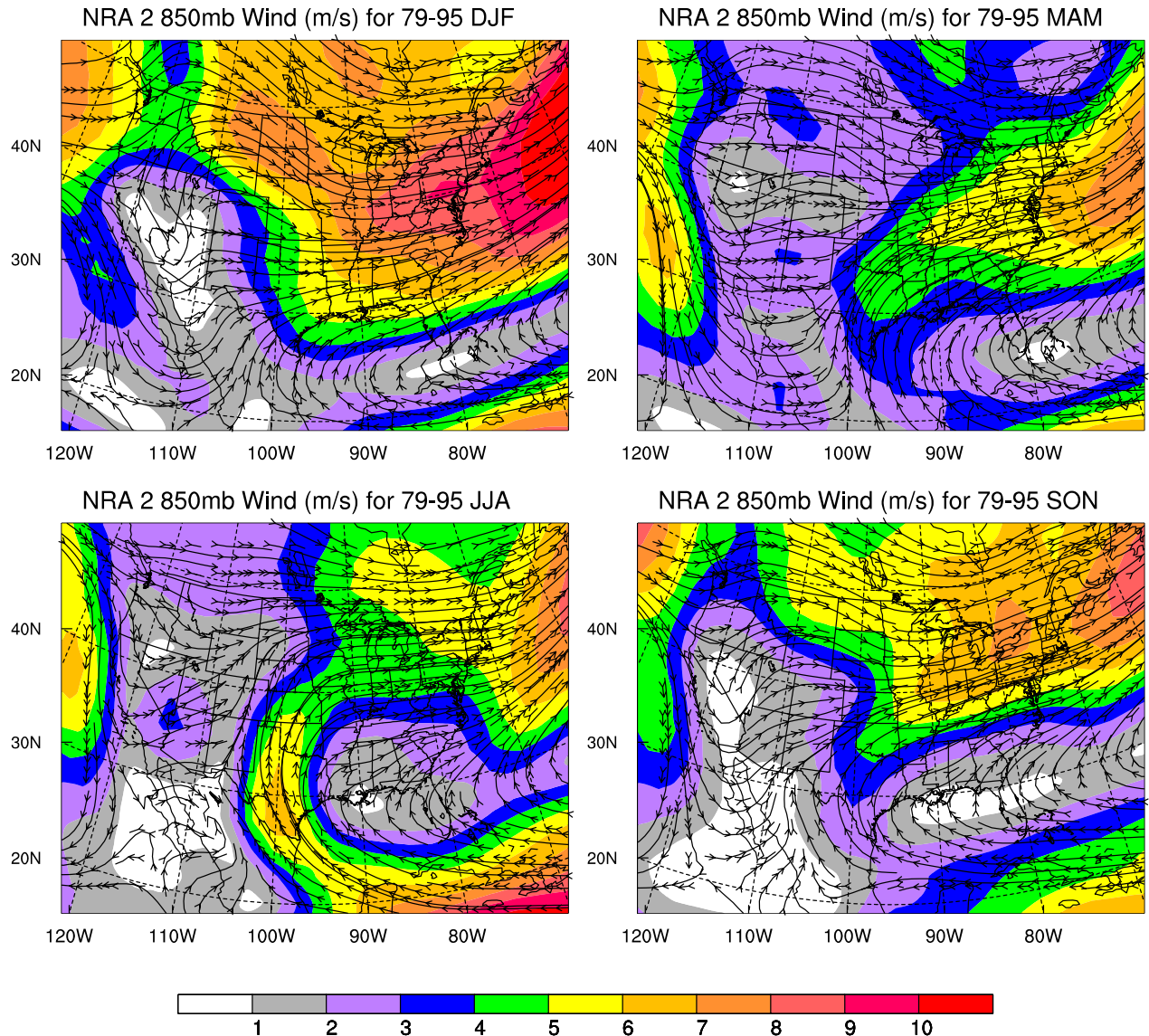


Figure 2. Map of observed (1979-1995) wind flow at a level of 850 hPa for winter (top left), spring (top right), summer (bottom left), and fall (bottom right). Barbed lines indicated wind flow directions and colored shading indicates speed ( $\text{m s}^{-1}$ ).

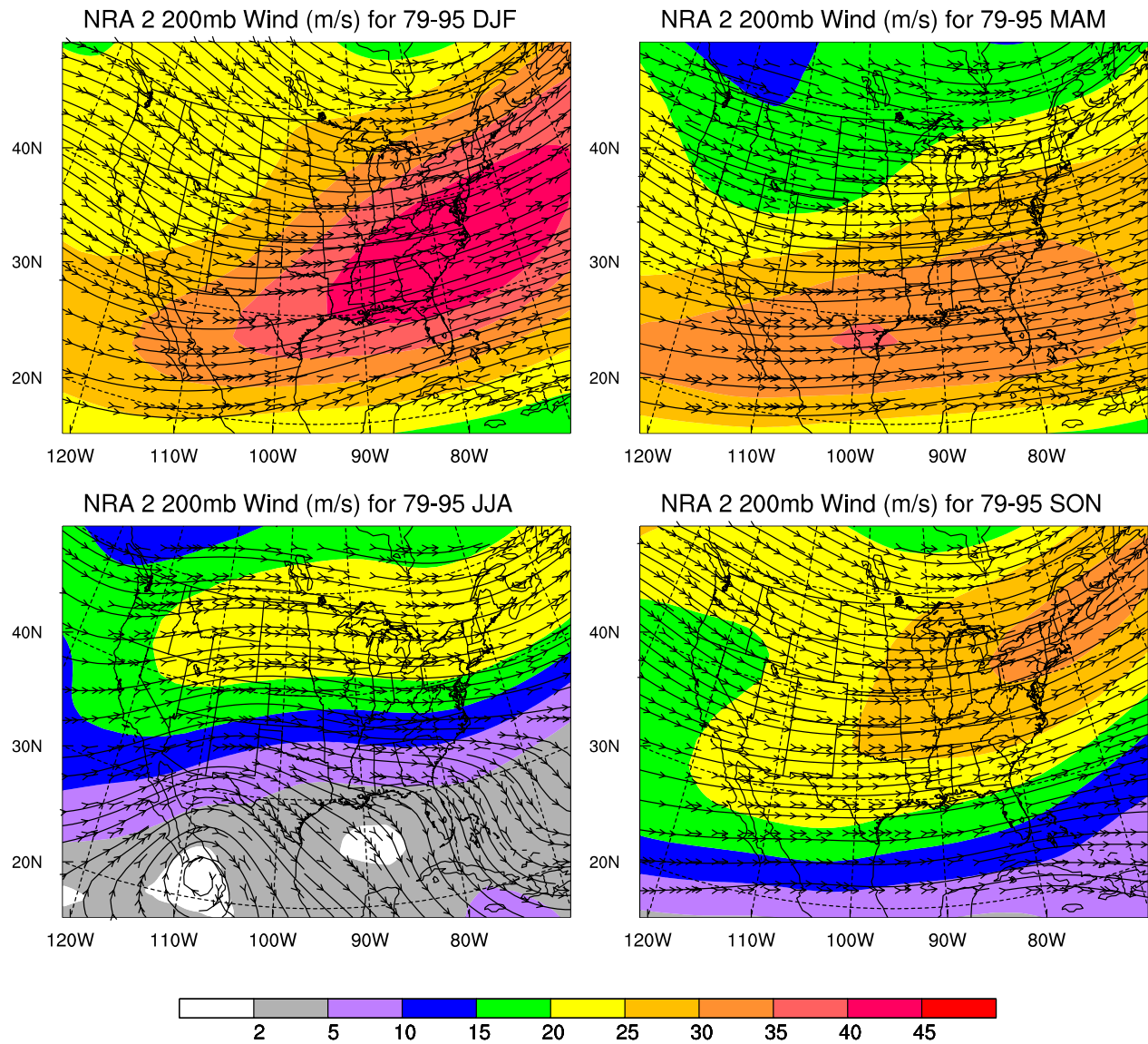


Figure 3. Map of observed (1979-1995) wind flow at a level of 200 hPa for winter (top left), spring (top right), summer (bottom left), and fall (bottom right). Barbed lines indicated wind flow directions and colored shading indicates speed ( $\text{m s}^{-1}$ ).

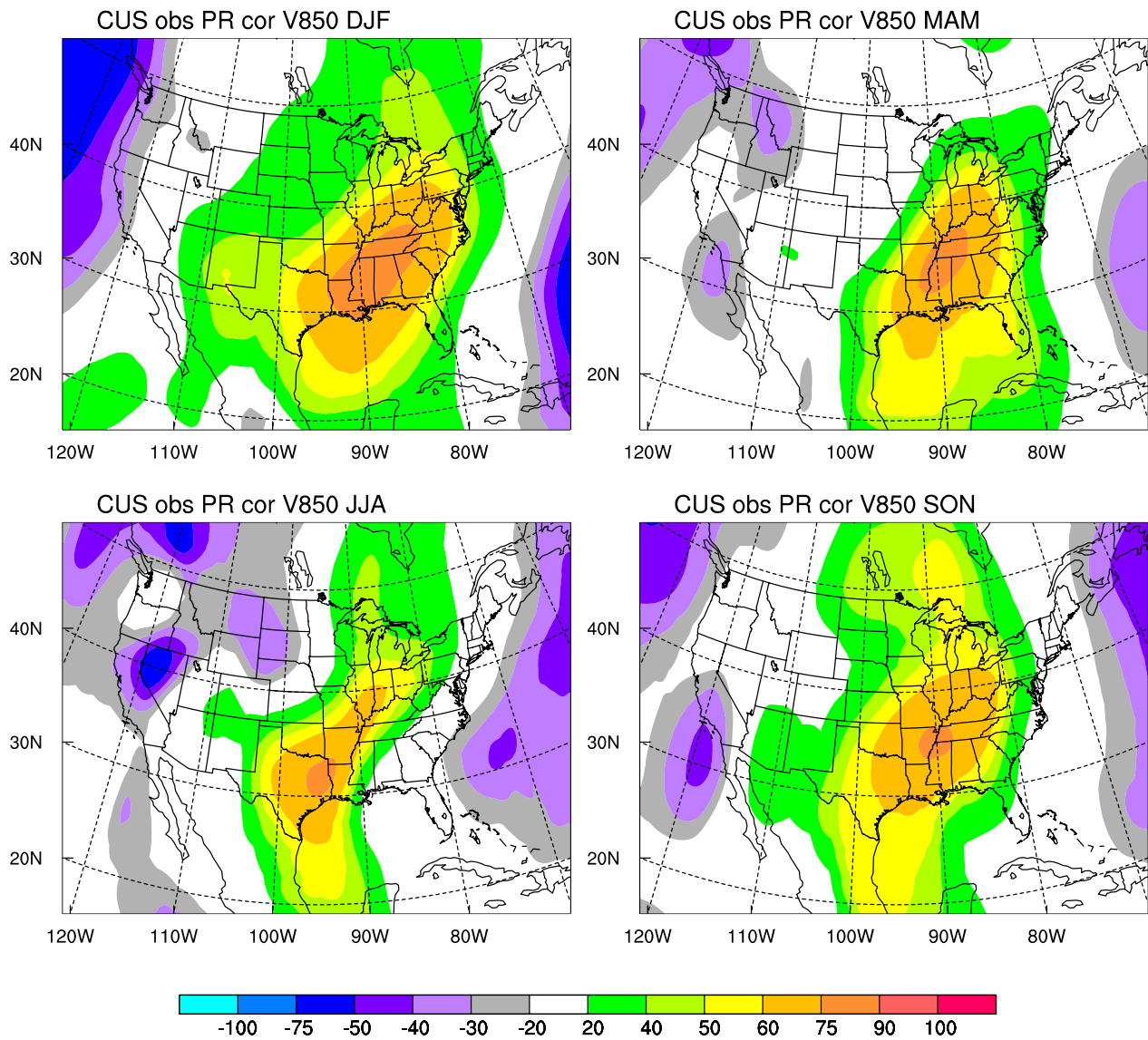


Figure 4. Maps of correlation coefficient for 1979-1995 between observed southerly component of the wind speed at 850 hPa and observed precipitation in the central U.S. for winter (top left), spring (top right), summer (bottom left), and fall (bottom right).

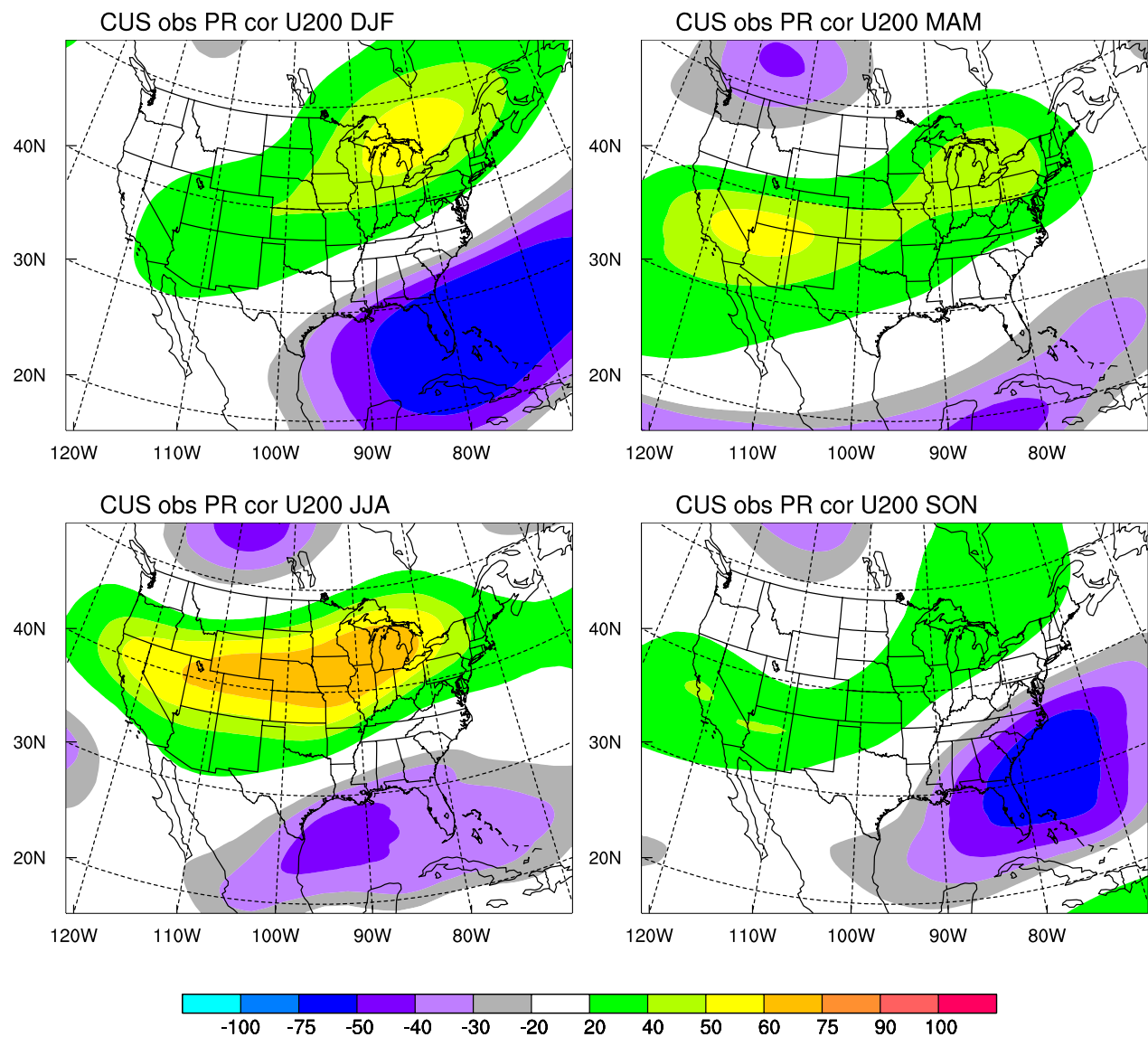


Figure 5. Maps of correlation coefficient for 1979-1995 between observed westerly component of the wind speed at 200 hPa and observed precipitation in the central U.S. for winter (top left), spring (top right), summer (bottom left), and fall (bottom right).

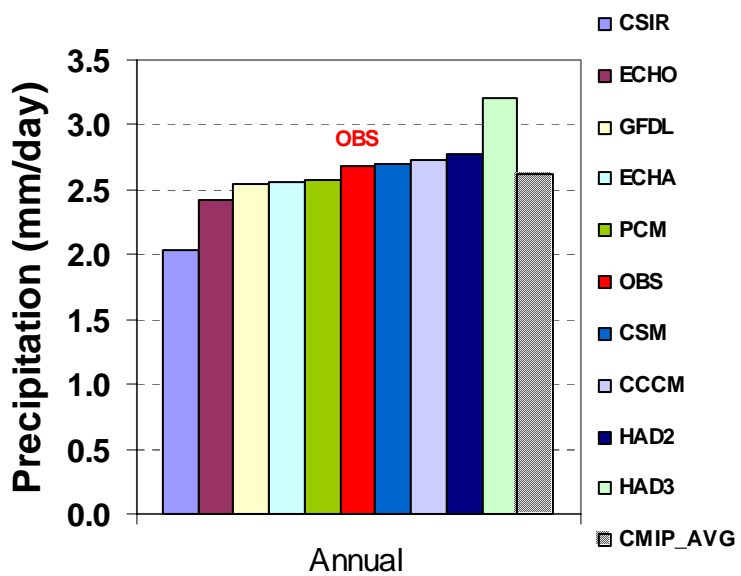


Fig. 6. Annual precipitation for the observations (1979-1995) and the control simulations of CMIP models.

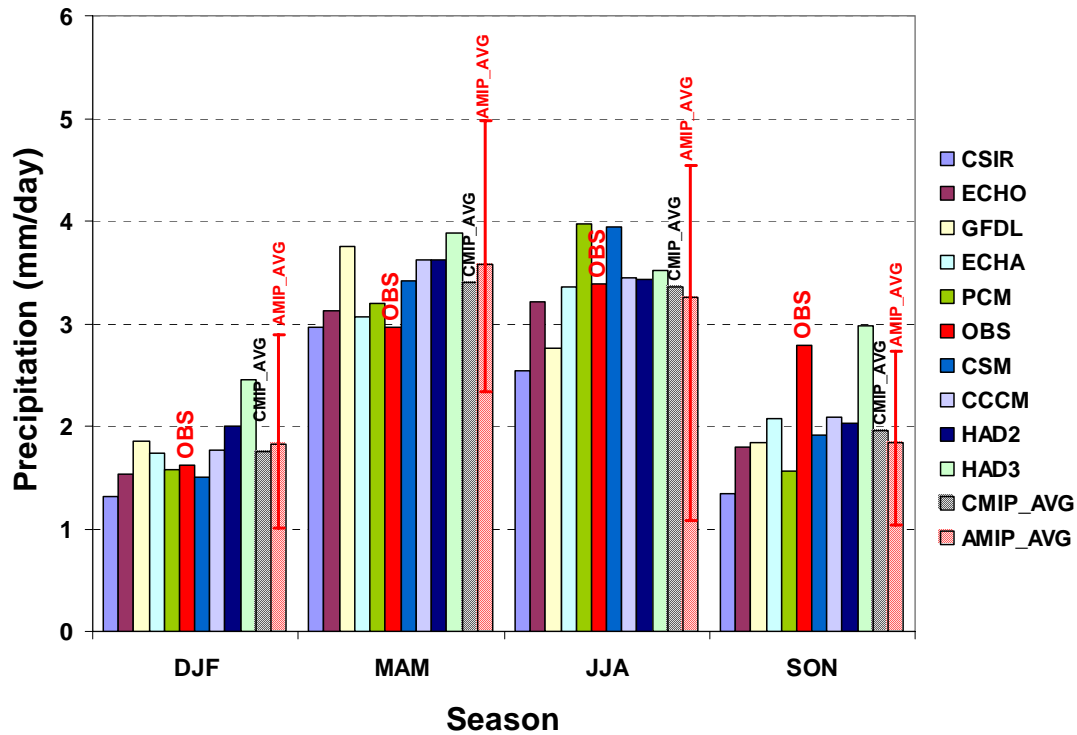


Fig. 7. Seasonal precipitation for the observations (1979-1995), the control simulations of the CMIP models, and model means of all CMIP and AMIP models. For the AMIP results, the maximum and minimum model values are also displayed.

### Southerly component at 850 hPa in LLJ region

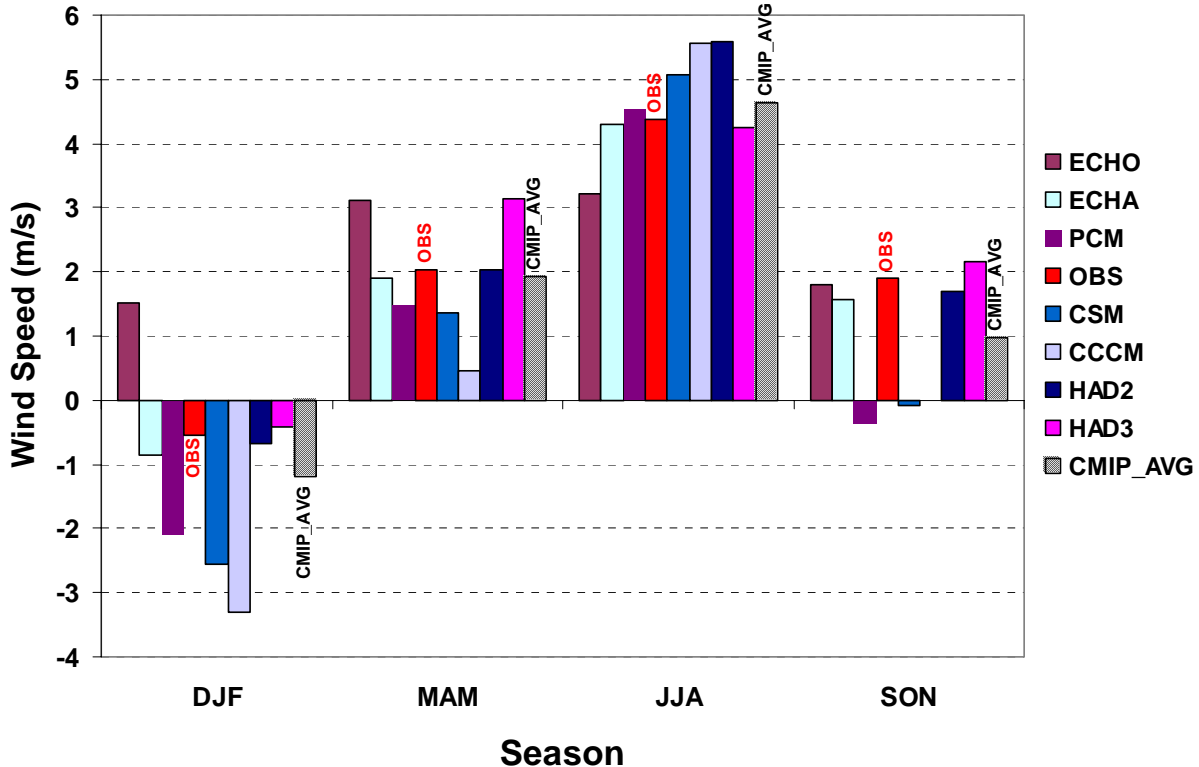


Figure 8. Southerly wind component ( $\text{m s}^{-1}$ ) at 850 hPa in the LLJ region for the 4 seasons for CMIP models (last 30 years of control run) and observations for the period 1979-1995. Model mean is also displayed.

### 850 hPa in LLJ region

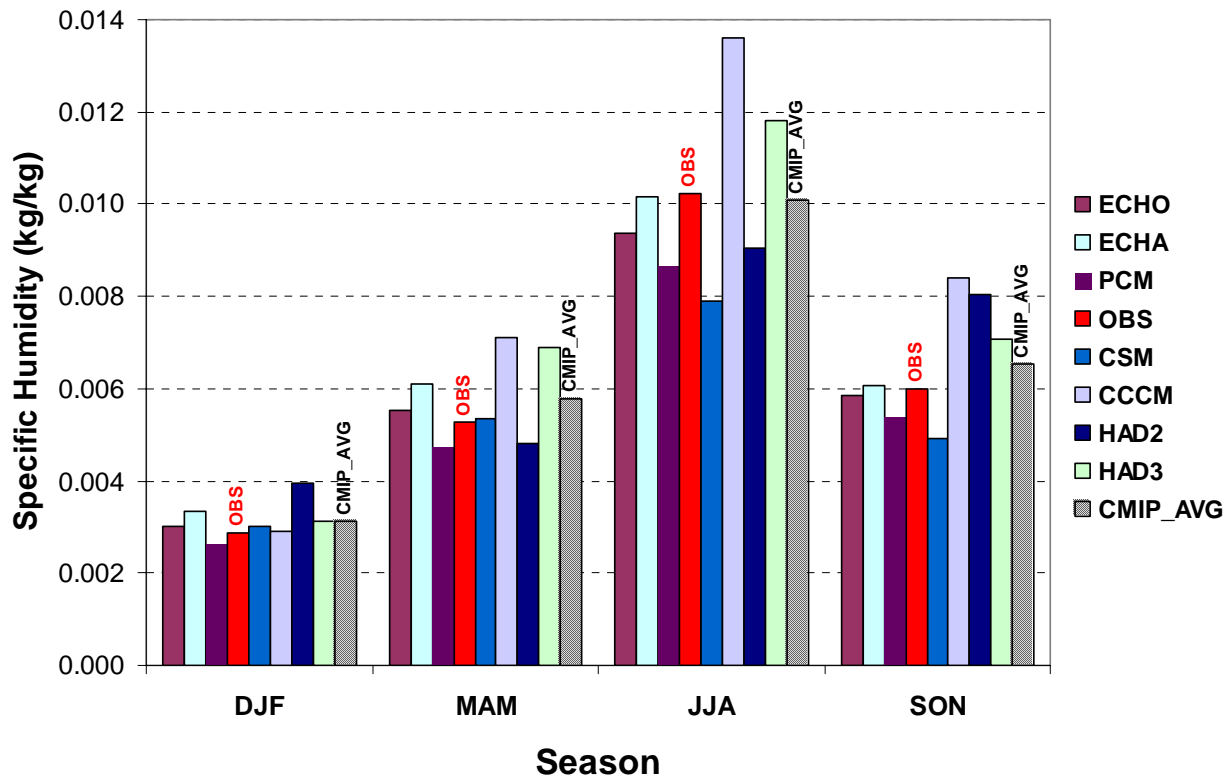


Fig. 9. Specific humidity at 850hPa of LLJ region for the four seasons for CMIP models (last 30 years of control run) and observations for the period 1979-1995. Model mean is also displayed.

### Precipitation vs V850 in LLJ region

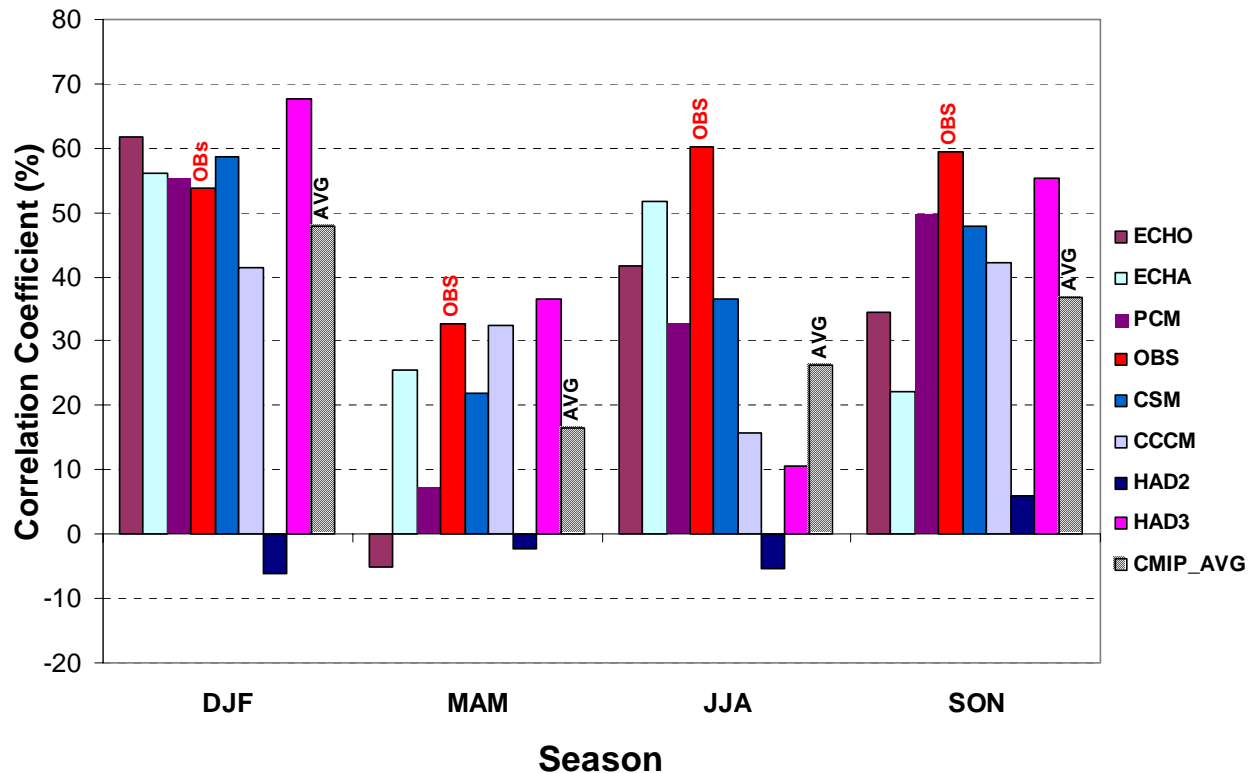


Fig. 10. Correlation between central US model precipitation and model southerly wind component in the LLJ region for CMIP models by season. Model mean is also shown.

### Precipitation vs U200 in IA region

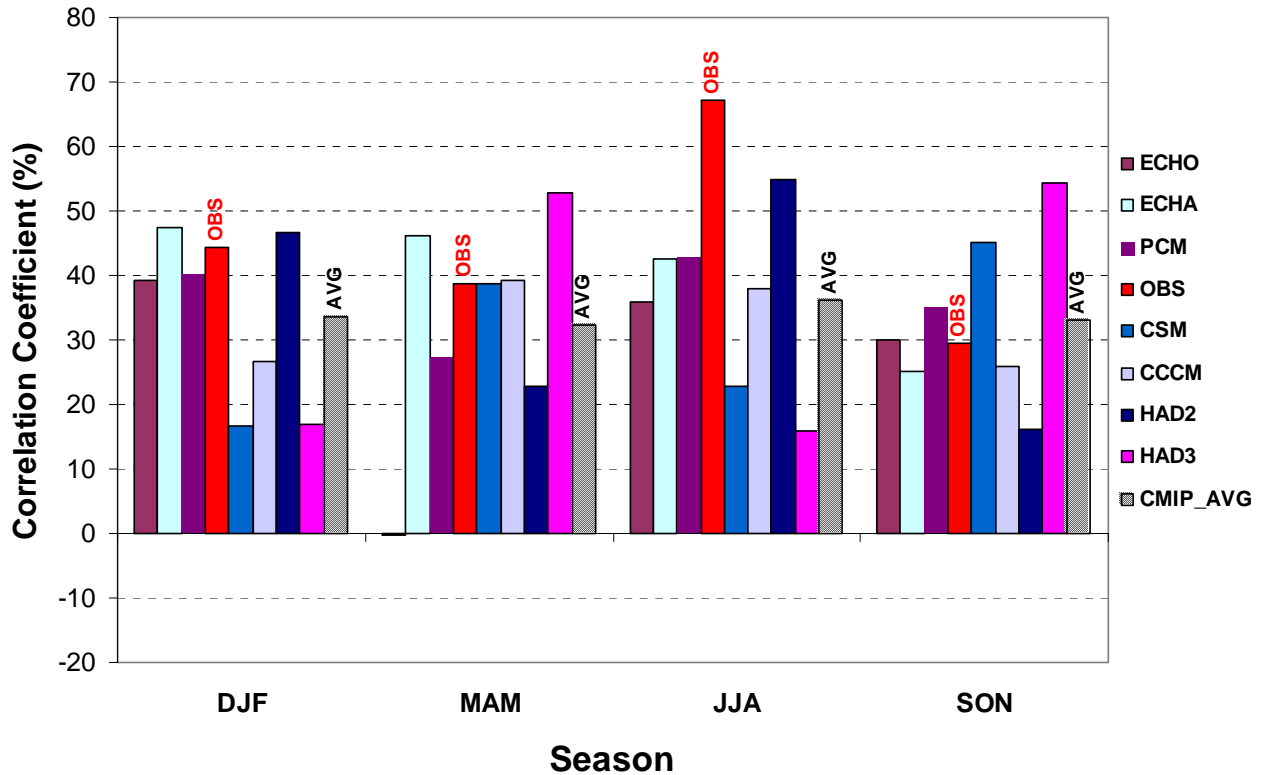


Fig. 11. Correlation coefficient for 4 seasons for CMIP models between model precipitation in the central U.S. and model westerly component of the wind speed at 200 hPa in the IA region. Model mean is also displayed.

### Precipitation vs U200 over CA region

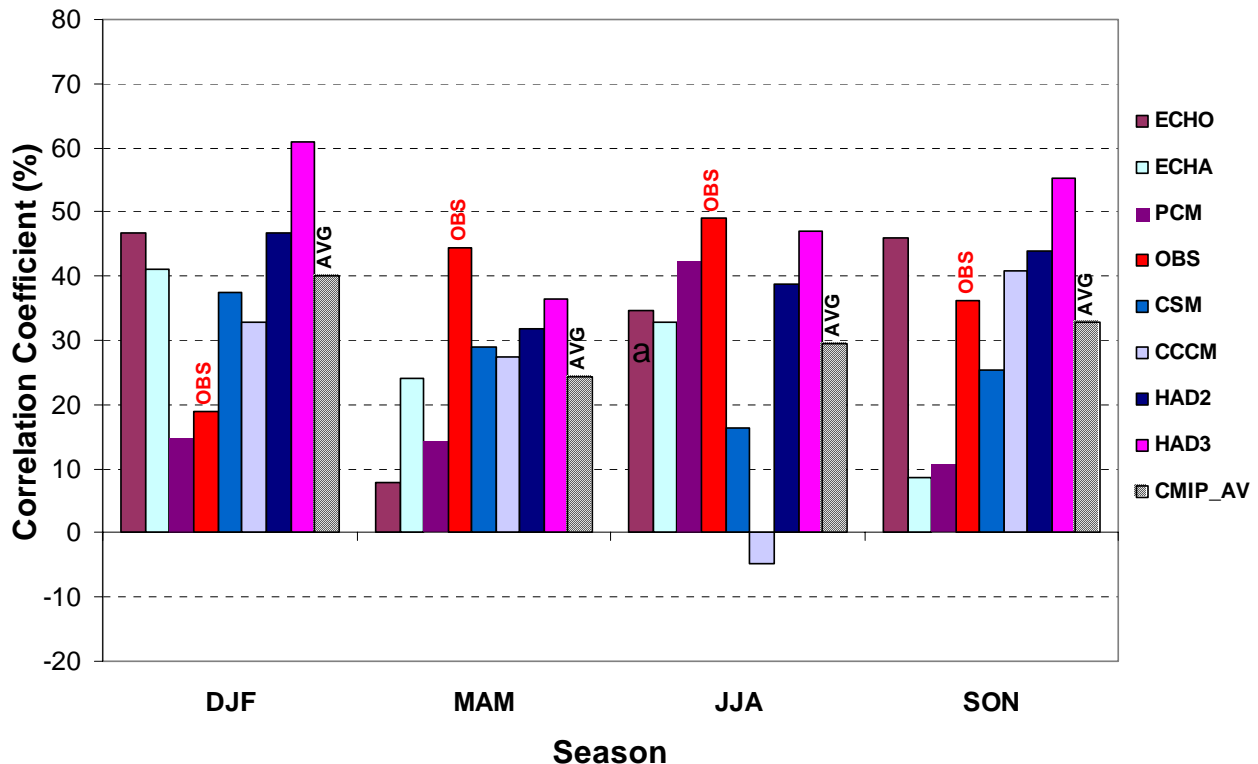


Figure 12. Correlation coefficient for 4 seasons for CMIP models between model precipitation in the central U.S. and model westerly component of the wind speed at 200 hPa in the CA region. Model mean is also displayed.

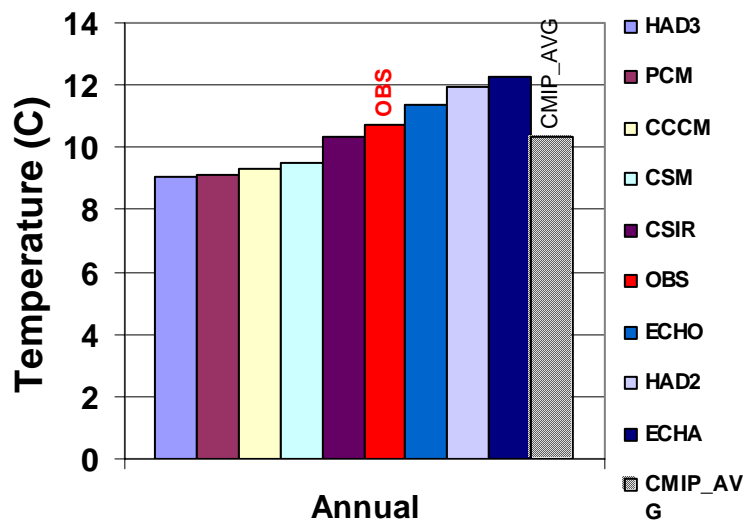


Fig. 13. Annual surface air temperature ( $^{\circ}\text{C}$ ) for the central U.S. for CMIP models and observations. The CMIP values were obtained from an average of the last 30 years of each model's control run. The observed value is for the period 1979-1995. The model mean is also displayed.

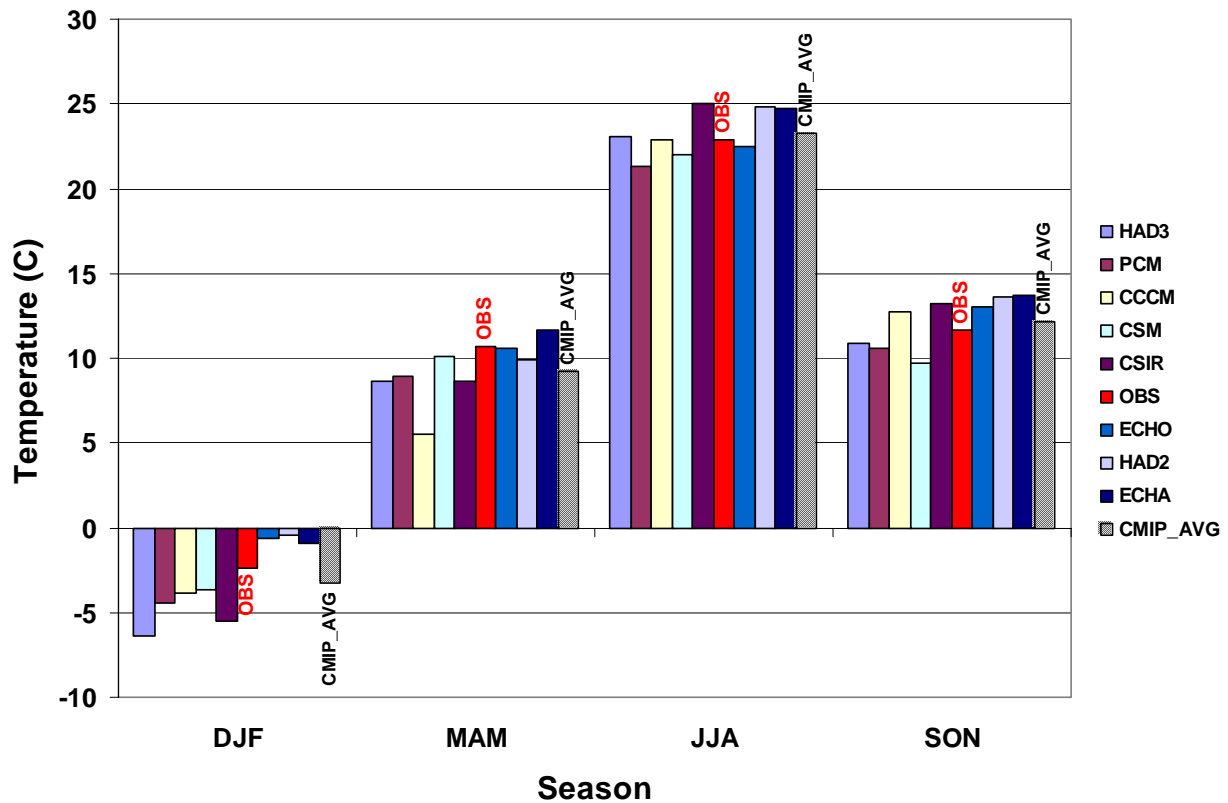


Figure 14. Seasonal mean surface air temperature ( $^{\circ}\text{C}$ ) for the central U.S. for CMIP models and observations. The CMIP values were obtained from an average of the last 30 years of each model's control run. The observed value is for the period 1979-1995.

### Transient-Control (Central US)

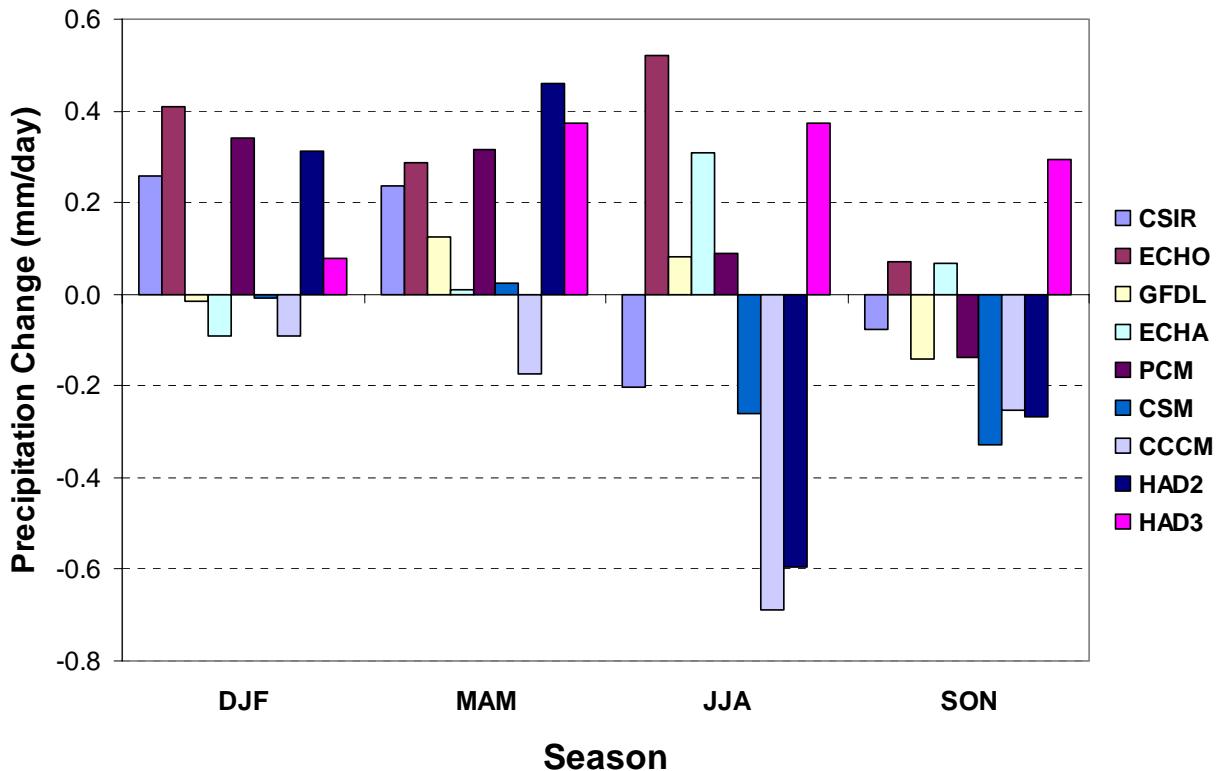


Figure 15. Precipitation changes in the transient runs of the CMIP models for the central U.S. The change is the difference between the average of years 65-75 in the transient run and the average of the last 30 years of the control run.

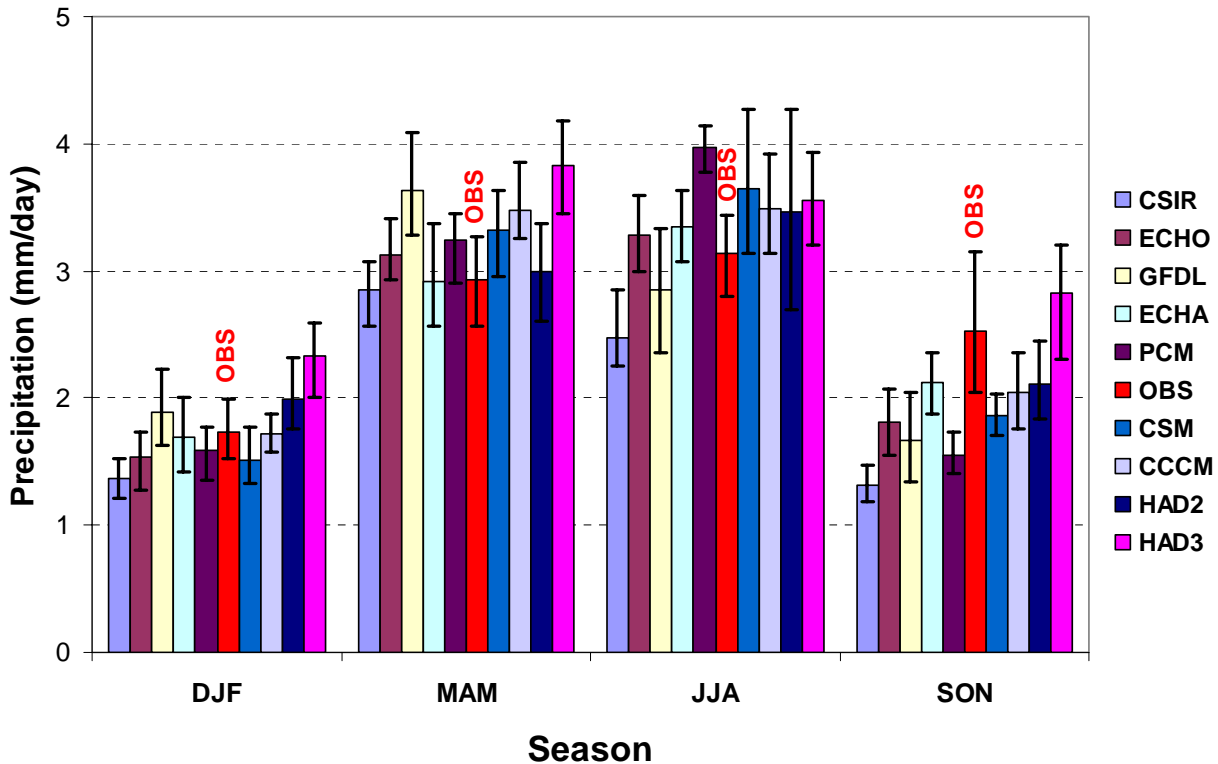


Figure 16. The mean, maximum, and minimum values of a 11-year running average of the control run and mean, maximum, and minimum values of a 11-yr running average of the 20<sup>th</sup> Century (1900-1999) observations for central US precipitation for the four seasons. The mean is indicated by the bar height while the maximum and minimum limits are denoted by the vertical line.

### Transient - Control (Central US)

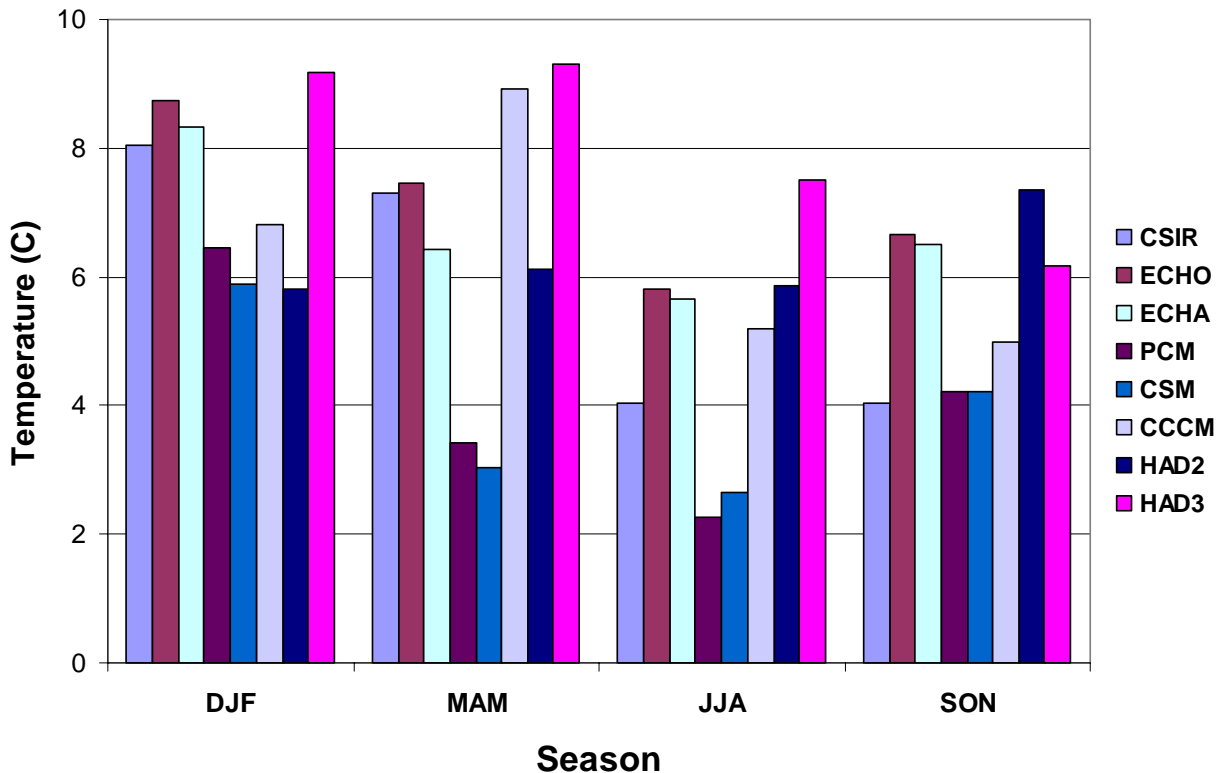


Fig. 17. Surface air temperature changes ( $^{\circ}\text{C}$ ) in the transient runs of the CMIP models for the central U.S. The change is the difference between the average of years 65-75 in the transient run and the average of the last 30 years of the control run.

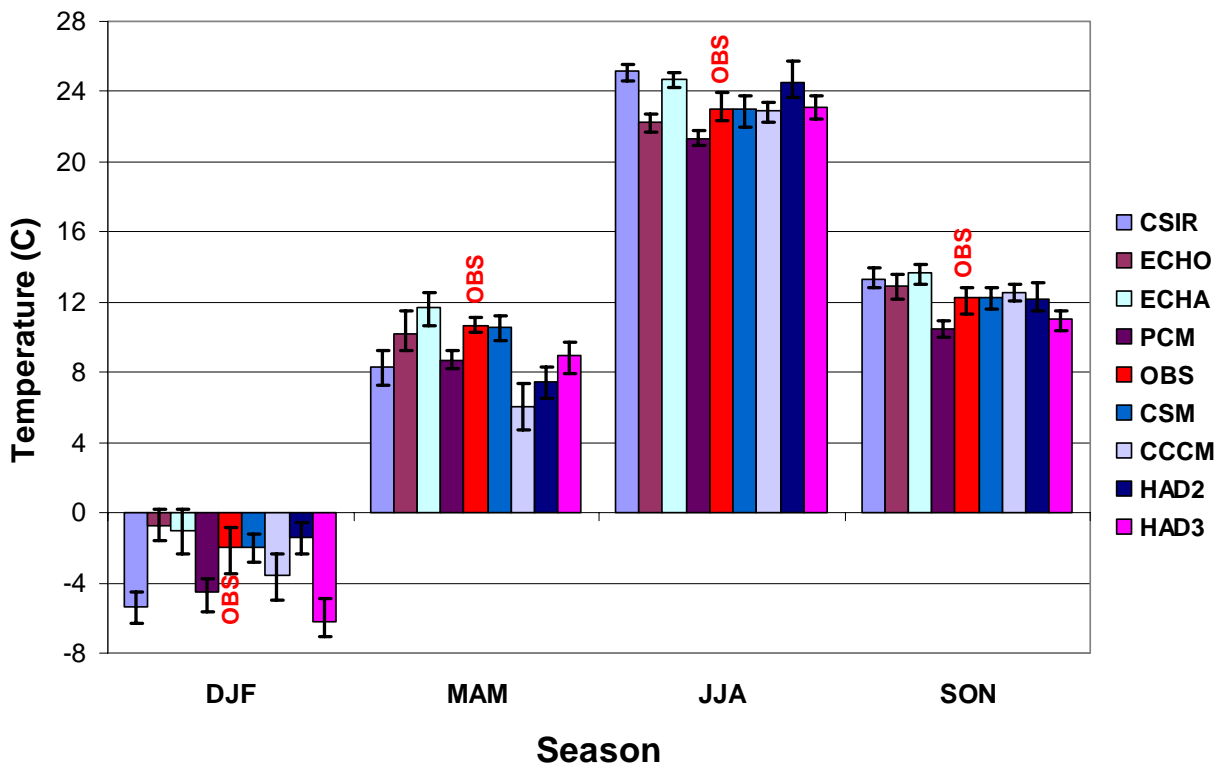


Figure 18. The mean, maximum, and minimum values of a 11-year running average of the control run and mean, maximum, and minimum values of a 11-yr running average of the 20<sup>th</sup> Century observations for central US surface air temperature for the four seasons. The mean is indicated by the bar height while the maximum and minimum limits are denoted by the vertical line.

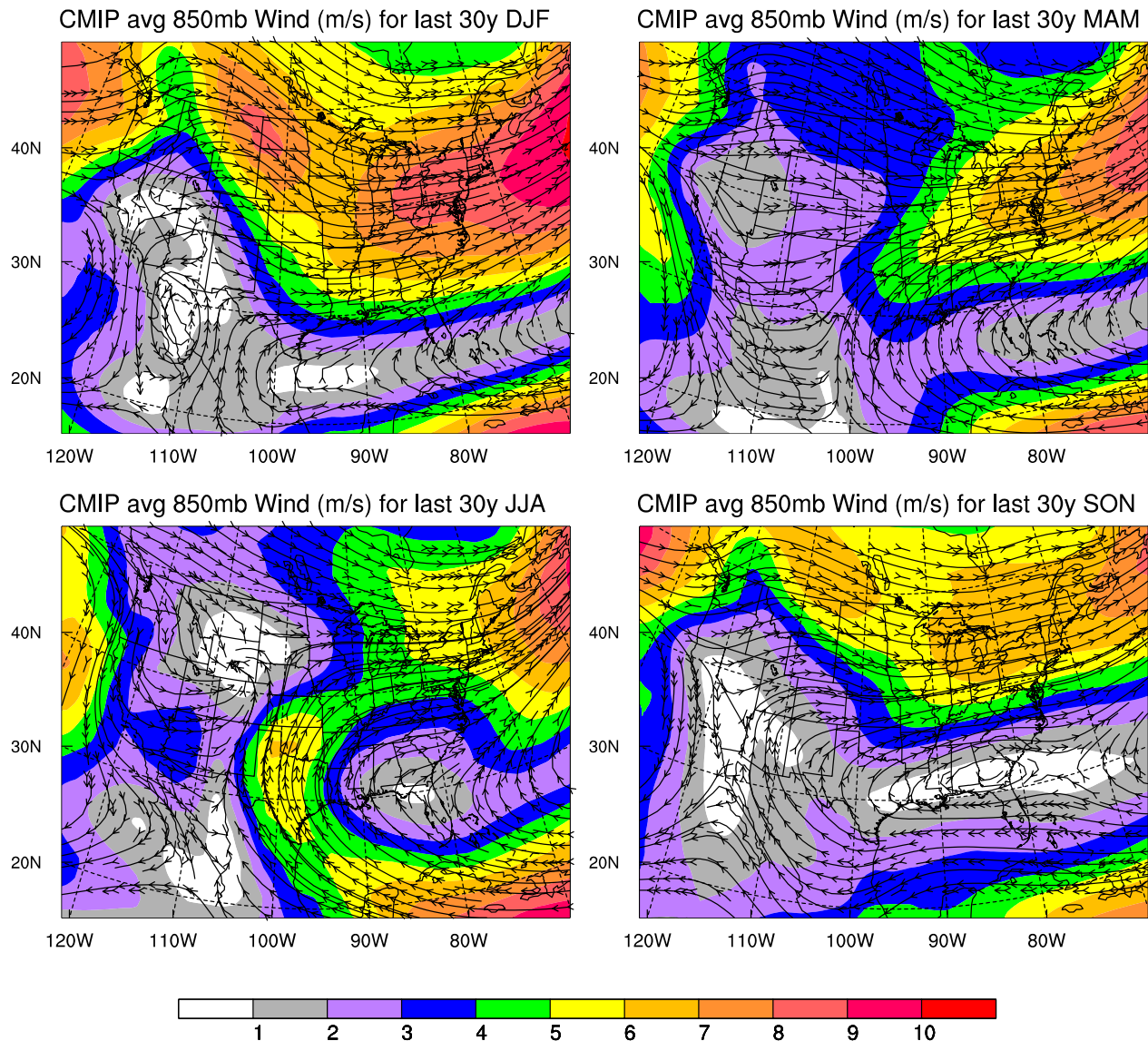


Figure 19. CMIP model composite maps of wind flow at a level of 850 hPa for (top left) winter, (top right) spring, (bottom left) summer, and (bottom right) fall. Barbed lines indicated wind flow directions and colored shading indicates speed ( $\text{m s}^{-1}$ ).

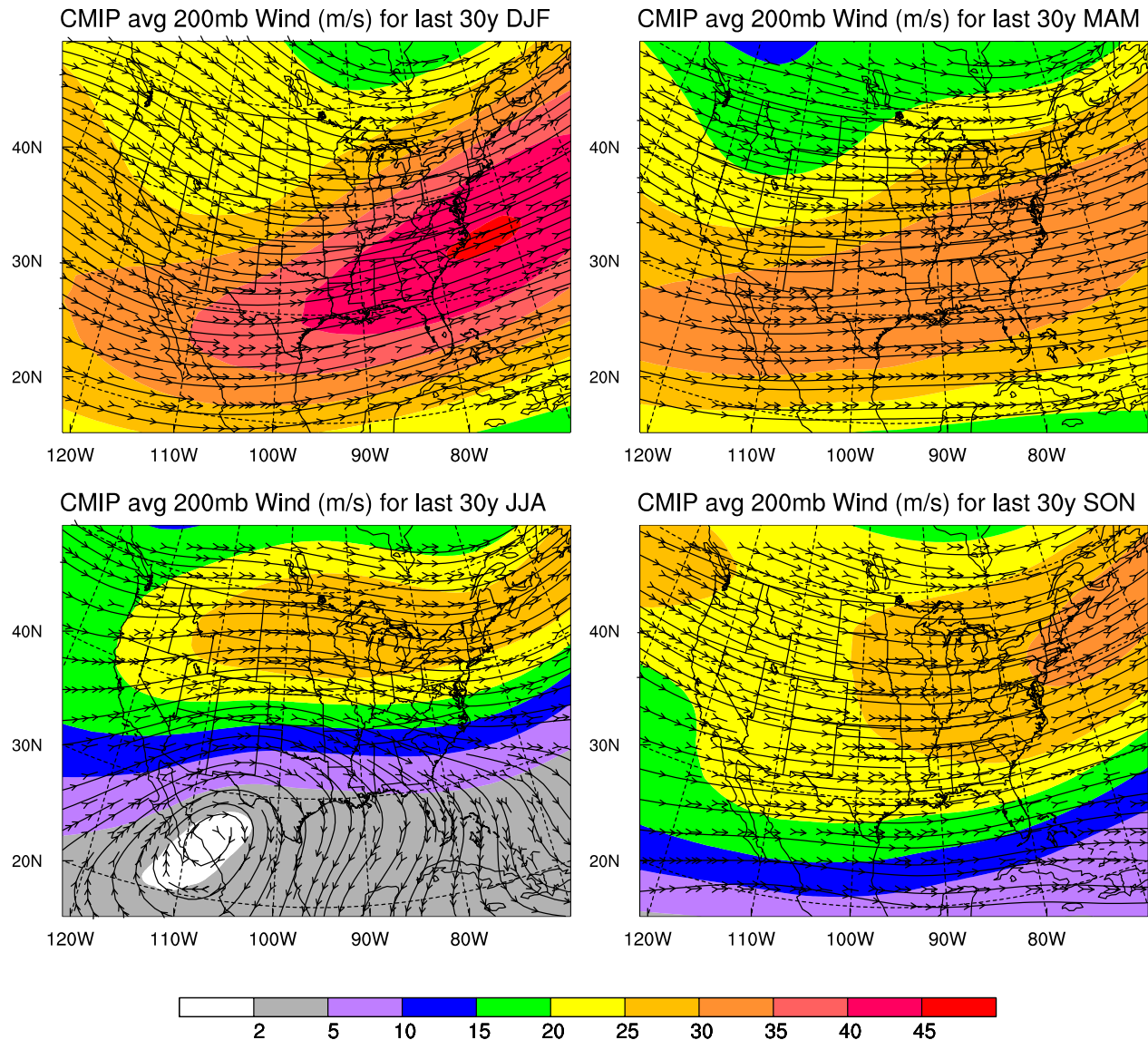


Figure 20. CMIP model composite maps of wind flow at a level of 200 hPa for (top left) winter, (top right) spring, (bottom left) summer, and (bottom right) fall. Barbed lines indicated wind flow directions and colored shading indicates speed ( $\text{m s}^{-1}$ ).

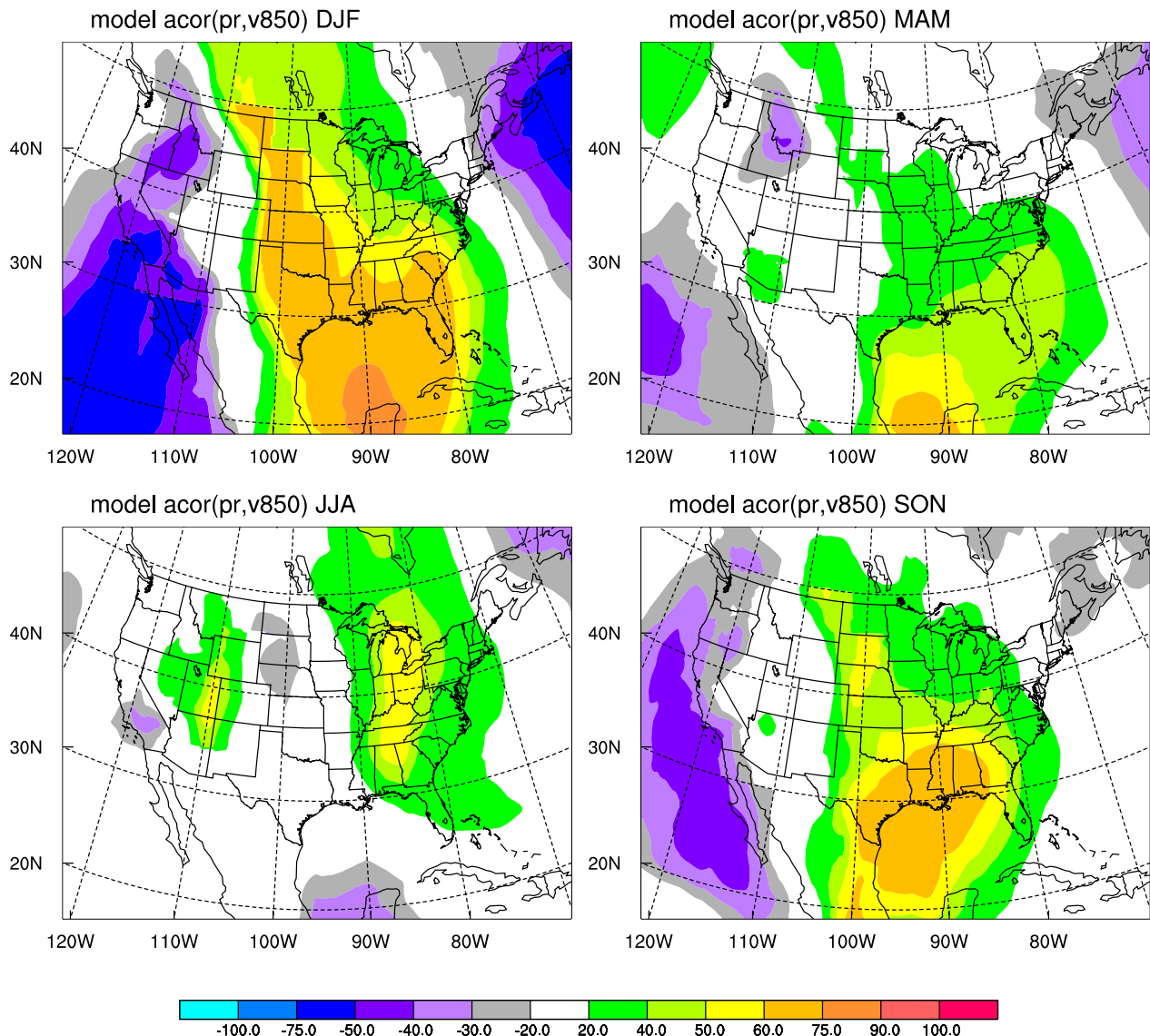


Figure 21. AMIP model composite maps of correlation coefficient between southerly component difference (model-observed) of the wind speed at 850 hPa and precipitation difference (model-observed) in the central U.S. for 4 seasons.

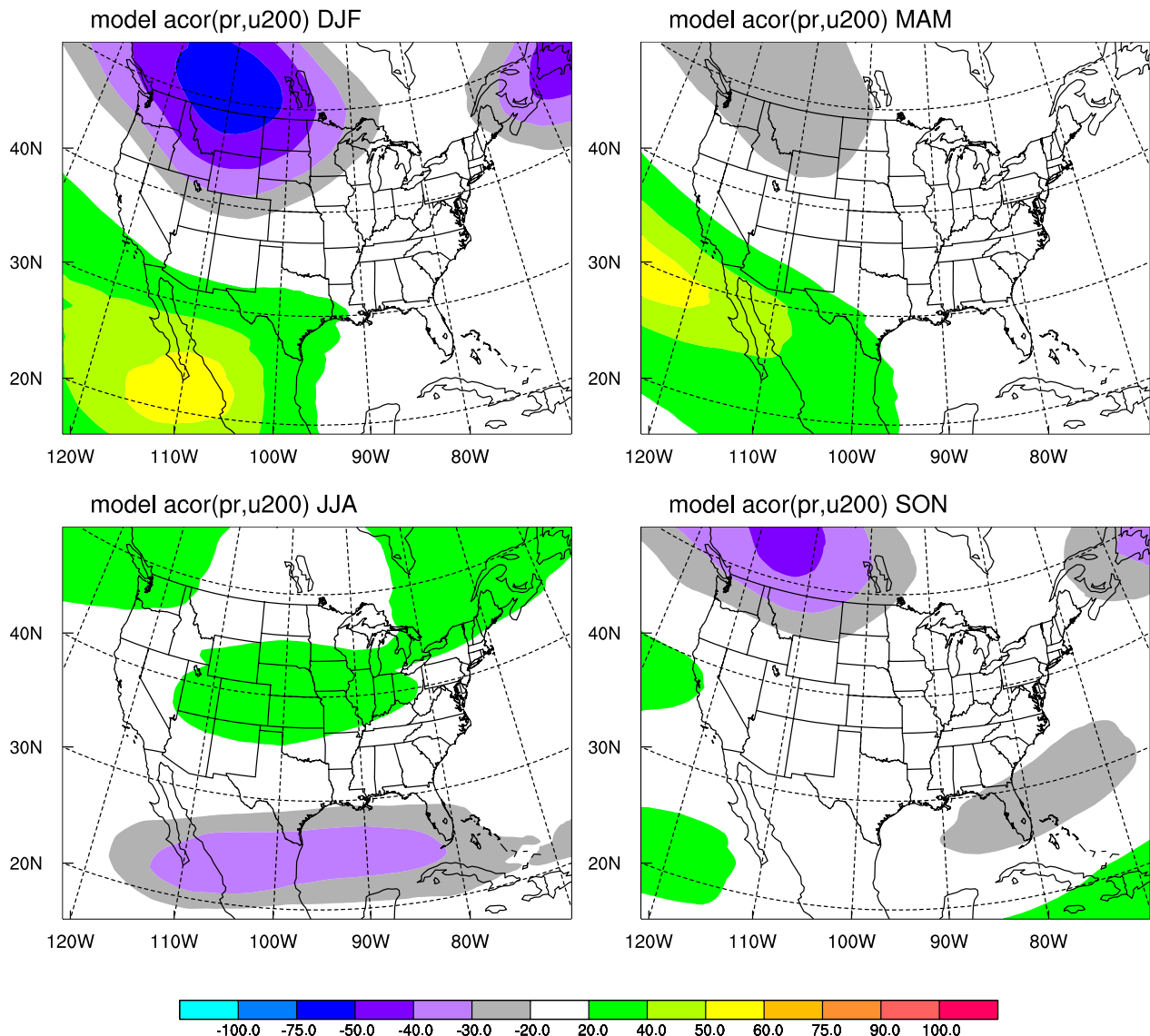


Figure 22. AMIP model composite maps of correlation coefficient between southerly component difference (model-observed) of the wind speed at 200 hPa and precipitation difference (model-observed) in the central U.S. for 4 seasons.